J. COMBIN. MATH. COMBIN. COMPUT. 127a (2025) 9407--9423

Journal of Combinatorial Mathematics and Combinatorial Computing
www.combinatorialpress.com/jcmcc

Combinatorial Press

Quantification of ultra-short-term forecasting performance of wind power based on multivariate LSTM and logistic coupled models

Zhihao Pan[1,✉], Zhenyu Fu[1], Guiquan Lin[1], Tao Wu[1], Zhifeng Yang[1], Xiao Teng[2]

[1] *Zhanjiang Power Supply Bureau of Guangdong Power Grid Co., Ltd., Zhanjiang, Guangdong, 524000, China*
[2] *College of Energy and Electrical Engineering, Hohai University, Nanjing, Jiangsu, 211100, China*

ABSTRACT
The power optimization of wind farms and the optimal control of wind turbines require high-precision power ultra-short-term prediction for each wind turbine. In order to improve the performance of ultra-short-term prediction of wind power, this paper couples the LSTM model with the Logistic model and combines it with Graph Convolutional Neural Network (GCN) to construct the ultra-short-term prediction model of wind power based on Logistic-LSTM-GCN, and test and analyze the prediction performance of the model. Comparing the LASSO, XGboost, LSTM, GRU and TCN-LSTM models, the MAE and RMSE of this paper's model are the lowest among all the models, which are 3.34% and 5.89%, respectively, and the R^2 is the highest, which is 79.76%. And the MAE and RMSE predicted by the model with inputs of four-dimensional spatio-temporal feature matrix are smaller than the model with inputs of one and two dimensions, and the R^2 value is larger than that of one and two-dimensional model. It indicates that the Logistic-LSTM-GCN model based on spatio-temporal information can extract the spatio-temporal information of wind farms more effectively, which improves the accuracy of wind cluster power prediction. In addition, with the increasing time step, the error indicators MAE, MAPE and RMSE are gradually increasing. Taking a time step of 4s for prediction, the prediction error of the model is minimized when considering multivariate variables such as wind speed, wind speed decomposition component, yaw error, wind direction, and rotor speed. This indicates that the multivariate LSTM, logistic and GCN coupled model can significantly improve the performance of ultra-short-term prediction of wind power.

Keywords: LSTM, Logistic model, GCN, wind power ultra-short-term prediction

✉ Corresponding author.
E-mail address: tx18921934382@126.com (Z. Pan).
Received 15 January 2024; Revised 20 February 2024; Accepted 30 November 2024; Published Online 15 April 2025.
DOI: 10.61091/jcmcc127a-524

1. Introduction

With the transformation of the global energy structure and the deepening of the concept of sustainable development, wind power, as a clean and renewable form of energy, is receiving more and more attention and emphasis. The accurate prediction of wind power is of vital significance to the stable operation of the power system, the effective utilization of energy and the economic operation of wind farms. Therefore, the study of wind power ultra-short-term prediction method has become a hot topic in the current energy field [1-4].

Ultra-short-term prediction of wind power refers to the prediction of wind farm output power in the next few hours, which is based on the past data of wind speed, wind direction, meteorological conditions, etc., and utilizes mathematical models and algorithms to predict the power generated by wind farms in the future period [5-8]. Accurate wind power prediction can effectively guide the operation and management of wind farms, optimize the power generation plan, improve the power generation efficiency, and reduce the energy cost. At the same time, wind power prediction also plays an important role in the scheduling of the power system, the optimal configuration and stable operation of energy storage equipment [9-11]. Ultra-short-term wind power prediction is mainly based on the theoretical foundation of meteorology, aerodynamics, statistics and other disciplines. Wind power prediction technology in some foreign wind power developed countries in the development of earlier, and has formed a mature prediction technology and complete system [12-15]. While China's research in this area is relatively lagging behind, but the progress is faster, up to now, all the wind farms connected to the grid in China have been equipped with wind power prediction systems [16-17].

Literature [18] emphasizes the importance of wind power prediction and describes the application of deep learning in wind power prediction. A new gating mechanism is adopted in the LSTM network to improve the prediction accuracy of LSTM in wind power prediction. The experimental results indicate that the improved LSTM prediction model can improve the prediction accuracy of LSTM prediction model in ultra-short-term wind power prediction. Literature [19] proposed a BiGRU-based ultra-short-term wind power prediction method. By combining ED architecture with BiGRU time series modeling and FT-Attention in order to improve the accuracy of wind power prediction. The results show that the method has a good application prospect in ultra-short-term wind power prediction. Literature [20] proposes an ultra-short-term wind power segmentation prediction method based on extreme weather identification. The prediction performance of the method was verified by applying the data from Texas wind farms, and it effectively improved the prediction accuracy. Literature [21] proposes an ultrashort-term wind power prediction method based on multivariate empirical dynamic modeling, which is characterized by the fact that its effectiveness depends only on the potential context hidden in the sequence of state variables, so it can improve the prediction accuracy, and the experimental results also validate its effectiveness, and it is able to obtain a more ahead of the prediction results. Literature [22] proposed an ultra-short-term wind power prediction model based on CEEMDAN with adaptive noise and LSTM network with improved WOA optimization. By establishing the IWOA-LSTM prediction model and applying this hybrid model to the ultra-short-term wind power prediction of a wind farm, the effectiveness of the model was concluded after comparison. Literature [23] constructed a combined method combining LSTM and ARMA based on VMD. The application of total wind power generation through Elia database shows that the method of VMD-LSTM-ARMA is very practical for the prediction of wind power. Literature [24] not only outlines the recent research results, performance and possible future scope, but also synthesizes long-term, short-term and ultra-short-term wind power forecasting methods and further develops the classification of forecasting methods for comparative analysis. Literature [25] aims to critically elaborate on the currently proposed ultra-short-term wind power prediction methods. Accordingly, the joint power prediction methods under extreme weather scenarios are explored and their effectiveness is confirmed by wind farm examples, and future research directions are proposed. Literature [26] describes a combined forecasting method based on day-ahead NWP localization techniques. The NWP information and time windows are used to localize the time points with low accuracy of rolling WPP forecasts, and a hybrid method combining neural network and continuous methods is proposed to forecast future wind power output. The results show that the proposed method effectively improves the ultra-short-term prediction accuracy of wind power. Literature [27] proposed a method for ultra-short-term wind power prediction using long and short-term memory neural networks. The hyperparameters of the LSTM prediction model were determined using the Spearman rank correlation coefficient method, and the LSTM prediction model was validated based on the measured data. The results show that the method exhibits higher prediction accuracy relative to the traditional artificial neural network.

In this paper, three models, namely LSTM, Logistic and GCN, are coupled and the model inputs are set to be multivariate data such as wind speed, wind speed decomposition component, yaw error, wind direction, and rotor speed, to realize the effective prediction of ultra-short-term power of wind power. In order to evaluate the prediction performance of the model, the Logistic-LSTM-GCN model in this paper is first experimentally compared with five commonly used models, namely, LASSO, XGboost, LSTM, GRU and TCN-LSTM. Then, the performance of the model is tested from two perspectives, namely, time step and unit characteristics, to explore the variation of the model's prediction performance under different time steps and the influence of the unit characteristics with different combinations of variables on the model's prediction performance.

2. Logistic-LSTM-GCN based ultra-short-term prediction model for wind power generation

There are some shortcomings in forecasting with a single forecasting model, such as incomplete information sources and sensitivity to the form of model settings. Combined forecasting refers to the application of two or more forecasting models for forecasting, the combined use of the information provided by a single model, in the form of an appropriate weighted average to produce a combined forecasting model, as much as possible to improve the accuracy. There are linear combination models, optimal linear combination models, Bayesian combination models, transformation function combination models, econometric and system dynamics combination models, etc. In this paper, a linear combination model combining Logistic model, LSTM model, and GCN model is used for ultra-short-term prediction of wind power.

2.1. Logistic and LSTM model bases

2.1.1. Logistic model. Logistic model, which can also be called logistic regression model, is a generalized linear regression analysis model [28]. In this paper, the Logistic model is used to predict the ultra-short-term power of wind power, which is given by:

$$P(t)=\frac{KP_0e^{rt}}{K+P_0\left(e^{rt}-1\right)} \tag{1}$$

where t is time. K is the capacity, i.e., the limit that can be reached $P(t)$ by growing to the end. P_0 is the initial capacity, i.e., the number of $t=0$ moments. r is the growth rate, r the larger the growth is faster, the faster approaching K value, r the smaller the growth is slower, the slower approaching K value. After the establishment of the logistic model in this paper, the nonlinear least squares method is used to estimate the parameters of K, P_0, and r, and to predict the future data.

The Logistic model starts off with a roughly exponential growth in the initial stages. Then the increase slows down as it begins to become saturated. Logistic models are commonly used in the fields of data mining, automatic disease diagnosis, economic forecasting, and so on.

2.1.2. LSTM model. LSTM is a temporal recurrent neural network specifically designed to solve the long-term dependency problem that exists in general recurrent neural networks (RNNs) [29]. LSTM avoids the problem of gradient vanishing or gradient inflation by increasing the input thresholds, forgetting thresholds, and output thresholds, so that the weights are changing during the self-looping process. Due to its unique design structure, LSTM is suitable for processing and predicting important events with intervals and delays in the time series.

The LSTM unit structure flow is shown in Fig. 1, where A module is the unit structure of LSTM. Assuming that h_i is the output value of the state at moment i, x_i is the input value at moment i, W denotes the weight matrix of the corresponding gate, and b denotes the bias of the corresponding gate, the specific flow of LSTM is:

1) Forgetting threshold: combine the network output of the previous moment with the network input of the current moment, and then perform a linear transformation through the sigmoid activation function, and map the result to 0~1 as the memory attenuation coefficient f_t, where 1 means "complete acceptance" and 0 means "complete ignorance", the formula is as follows:

$$f_t = \sigma\left(W_f \cdot \left[h_{t-1}, x_t\right] + b_f\right) \tag{2}$$

2) Input threshold: determine what new information needs to be saved in the cell state. First, the coefficient i_t of the input threshold is obtained using a method similar to the calculation of the memory decay coefficient, after which the learned memory $\tilde{C}_t$ of the current state is obtained by a linear transformation and the tanh activation function, which is given by the two-step equation:

$$i_t = \sigma\left(W_i \cdot \left[h_{t-1}, x_t\right] + b_i\right) \tag{3}$$

$$\tilde{C}_t = \tanh\left(W_C \cdot \left[h_{t-1}, x_t\right] + b_C\right) \tag{4}$$

3) Cell state update: For the previous moment state C_{t-1} multiplied by its attenuation coefficient f_t, plus the memory learned under that moment $\tilde{C}_t$ multiplied by its attenuation coefficient i_t, to get the state update value, Eq:

$$C_t = f_t \times C_{t-1} + i_t \times \tilde{C}_t \tag{5}$$

4) Output threshold: firstly, the coefficient o_t of the output threshold is obtained by the method similar to the calculation of the memory decay coefficient, and then the output value is obtained by multiplying with the coefficient after inputting the cell state into tanh, which is given by the two-step formula:

$$o_t = \sigma\left(W_o \cdot \left[h_{t-1}, x_t\right] + b_o\right) \tag{6}$$

$$h_t = o_t \times \tanh\left(C_t\right) \tag{7}$$

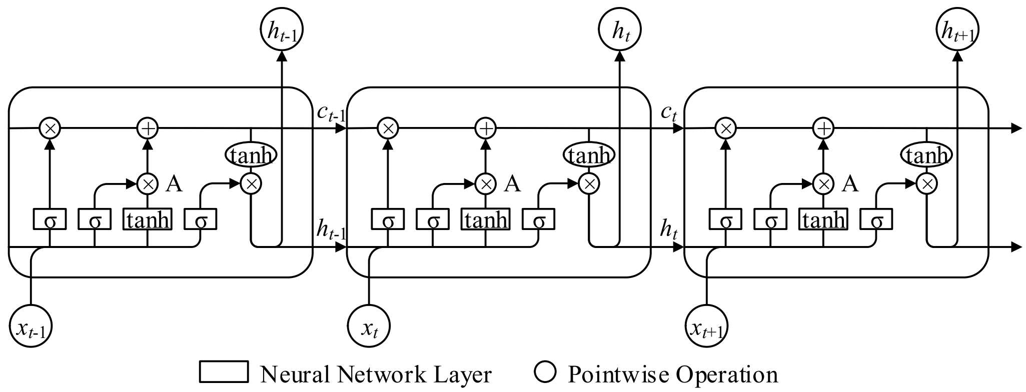

Fig. 1. Flow diagram of LSTM unit structure

2.2. Coupled LSTM and Logistic Prediction Models

Based on the above two models, in this paper, the prediction results of Logistic model and LSTM model are used to train the weight parameters by linear regression network. And the prediction is carried out in order to get better prediction results. The combined prediction model is defined as:

$$\hat{y} = x_1 w_1 + x_2 w_2 + b \tag{8}$$

where model output $\hat{y}$ is the prediction of the true cumulative number of diagnosed patients, x_1 is the result obtained from the LSTM model, x_2 is the result obtained from the Logistic model, w_1 and w_2 are the weights, and b is the bias.

The loss function is:

$$\begin{aligned} l(w_1, w_2, b) &= \frac{1}{n}\sum_{i=1}^{n} l^{(i)}(w_1, w_2, b) \\ &= \frac{1}{n}\sum_{i=1}^{n}\frac{1}{2}\left(x_1^{(i)} w_1 + x_2^{(i)} w_2 + b - y^{(i)}\right)^2 \end{aligned} \tag{9}$$

In model training, a set of model parameters, denoted as w_1^*, w_2^*, b^*, is found and small batch stochastic gradient descent is used to optimize the parameters to minimize the average loss of the training samples, Eq:

$$w_1^*, w_2^*, b^* = \underset{w_1, w_2, b}{\arg\min}\, l(w_1, w_2, b) \tag{10}$$

Small batch stochastic gradient descent is used to optimize the parameters, and the model parameters are iterated as follows:

$$\begin{cases} w_1 \leftarrow w_1 - \dfrac{\eta}{|\beta|}\displaystyle\sum_{i\in B}\dfrac{\partial l^{(i)}(w_1, w_2, b)}{\partial w_1} \\ w_2 \leftarrow w_2 - \dfrac{\eta}{|\beta|}\displaystyle\sum_{i\in B}\dfrac{\partial l^{(i)}(w_1, w_2, b)}{\partial w_2} \\ b \leftarrow b - \dfrac{\eta}{|\beta|}\displaystyle\sum_{i\in B}\dfrac{\partial l^{(i)}(w_1, w_2, b)}{\partial b} \end{cases} \tag{11}$$

where $|\beta|$ denotes the number of samples in each small batch, η is called the learning rate, η too large may lead to oscillations and fail to converge, and η too small will lead to slow convergence, so it is crucial to choose an appropriate value of η.

The structure of the established Logistic-LSTM combined prediction model is shown in Fig. 2, in which the LSTM model has four layers of the network: input layer, LSTM layer, fully connected layer, and regression output layer, in which the LSTM layer is set to have 200 implied units.The prediction results of the Logistic model and the LSTM model are used as two inputs to the linear regression network, and the outputs of this combined prediction model are trained by the linear regression network. After this combined prediction model, the output result is the prediction result of this combined prediction model.

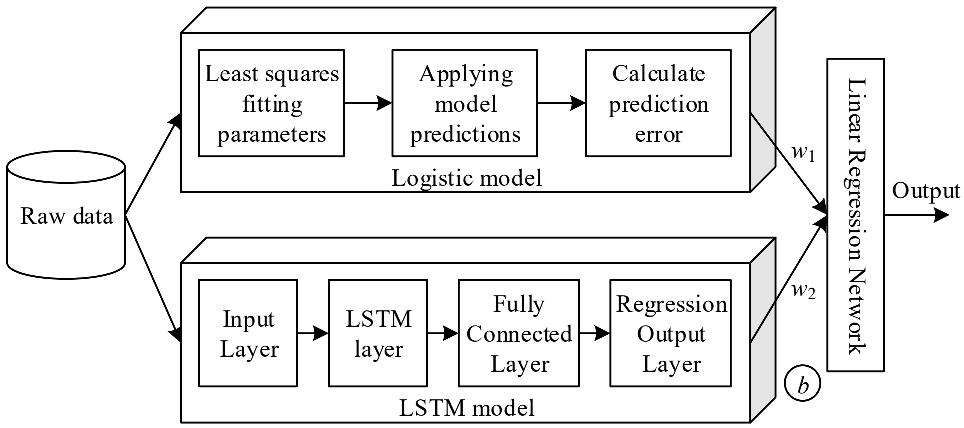

Fig. 2. Structure of Logistic-LSTM combined prediction model

2.3. Ultra-short-term prediction model for wind farms incorporating GCN

In order to further improve the accuracy of the ultra-short-term prediction of wind power, it is necessary to comprehensively consider the time-series correlation of wind speed, the spatial correlation of wind farms, and the station loss. Therefore, in this paper, based on the combined Logistic-LSTM prediction model, a GCN neural network [30] is introduced to solve the spatial correlation problem of wind farms and the station loss problem, while the temporal correlation problem is solved by the LSTM network, and ultimately, a deep spatio-temporal network of the ultra-short-term prediction model of wind power is constructed.

The model has four layers of neural networks, in which the first layer is a Logistic-LSTM network, the input is the data of key historical moments in the wind farm, and the output is a vector containing temporal features. The second layer is a GCN network, which builds a graph model with the correlation of spatial locations between WTGs, and combines the data output from the Logistic-LSTM network layer to form the graph data as inputs, and then extracts information from neighboring nodes connected to each node and updates the state of that node, which is used for extracting the spatial information within the wind farm. The third layer is also a GCN network, which is used to solve the problem of loss in the wind farm station by constructing the topology map of the electrical connections of the wind turbines and combining it with the data composition graph data processed by the second layer of the network as input. The fourth layer is the full connectivity layer, which integrates the output data from the first three layers of the network as the power generation of the entire wind farm.

2.3.1. GCN networks address spatial correlation issues. The graph convolutional neural network utilizes the structural information of the edge-vertex connections of the WTG connectivity graph $\tilde{A}$ and the input data of each WTG H for feature extraction of the implicit graph information. The message propagation between layers is given by equation (12) and the feature aggregation between turbines is given by equation (13):

$$H^{(l+1)} = \sigma\left(\tilde{D}^{-\frac{1}{2}}\tilde{A}\tilde{D}^{-\frac{1}{2}}H^{(l)}W^{(l)}\right) \tag{12}$$

$$\begin{aligned}\left(\tilde{D}^{0.5}\tilde{A}\tilde{D}^{0.5}H\right)_i &= \left(\tilde{D}^{0.5}\tilde{A}\right)_i \tilde{D}^{0.5}H \\ &= \left(\sum_k \tilde{D}_{ik}^{0.5}\tilde{A}_i\right)\tilde{D}^{0.5}H \\ &= \tilde{D}_{ii}^{0.5}\sum_j \tilde{A}_{ij}\sum_k^{0.5}\tilde{D}_j \\ &= \tilde{D}_{ii}^{-0.5}\sum_j \tilde{A}_{ij}\tilde{D}_{ij}^{-0.5}H_j \\ &= \sum_j \frac{1}{\sqrt{\tilde{D}_{ii}\tilde{D}_{ij}}}\tilde{A}_{ij}H_j\end{aligned} \tag{13}$$

The spatial correlation between WTGs can be effectively solved by using GCN network. In the connection relationship between WTGs in a wind farm, the initial attribute of each node, i.e., the input, is the time-series feature vector of WTGs extracted after the LSTM network layer. After the first layer of GCN network, the historical operation information of the neighboring units of each WTG is fully aggregated, and the feature vector of each node is transformed into m dimensions, outputting $n \times m$ dimensions of data, so that the model takes into account both the temporal characteristics of the wind power and the spatial characteristics within the wind farm, and the output of this layer is the power generation of the WTGs.

2.3.2. GCN network to address station losses. Station losses also need to be taken into account when performing wind power over short term. The wind turbines in the wind farm are connected together through power lines after being boosted by box transformers, and finally boosted and connected to the grid through the main transformer of the wind farm. This process will inevitably produce line losses, box transformer losses, main transformer losses, etc., these are collectively referred to as station losses. Because the station loss is not through the grid connection point to send out part of the power, so the station loss does not belong to the wind farm can actually send out the power, in the wind farm power ultra-short-term prediction needs to be subtracted from this part of the power loss. However, the sources of in-station losses are diverse and difficult to estimate, which makes it difficult to eliminate the impact of direct calculation on its accuracy. Using the graph convolutional neural network, we can construct the electrical connection diagram of wind turbines of wind farms according to the main electrical wiring diagram of wind farms, and imply the characteristics of the losses in the station in the electrical connection diagram of wind turbines, so as to indirectly complete the computation of the losses of the converging lines, main transformers and box transformers in the wind farms.

The WTGs are abstracted as nodes in the second layer GCN graph topology, and the power transmission paths are abstracted as edges between nodes. The propagation process of the node's own attributes in the GCN network well simulates the loss of WTG generation power occurring in the power transmission process. The input of the second GCN layer is the output matrix $H_1 = R^{(n \times m)}$ of the first GCN layer, and the output features are the power generated by the WTGs in the wind farm, $H_2 = R^{(n \times m)}$. Finally, after the full connectivity layer, the node features H_2 of the n WTGs are used as inputs to output the power generated by the whole wind farm in the next 4 hours.

3. Analysis of model prediction performance

3.1. Comparison of model prediction performance

In order to verify the performance of the Logistic-LSTM-GCN-based ultra-short-term prediction model for wind power, this paper first performs an arithmetic analysis to compare the prediction performance of this model with other models.

In this paper, wind power data from 48 wind farms in Province J from February to September 2023 are used for simulation experiments. The total installed capacity is 5486.74 MW, and the temporal resolution of power and weather elements is 15 min. the September data in the dataset is used as the test set, and the data from February to August is used as the training set. The numerical weather forecast elements include four weather features: wind speed, wind direction, pressure, and temperature. The correlation between the four weather features and the predicted power is shown in Figure 3. The darker the color represents the closer the weather feature is to the trend of the power.

After analysis, the strong correlation feature screened out is wind speed, and wind direction, pressure and temperature are weak correlation features. In this paper, the strongly correlated feature, i.e., wind speed, is used as the third dimension of the input data, and wind direction, pressure and temperature are normalized and weighted according to the correlation size as the third dimension of the input data.

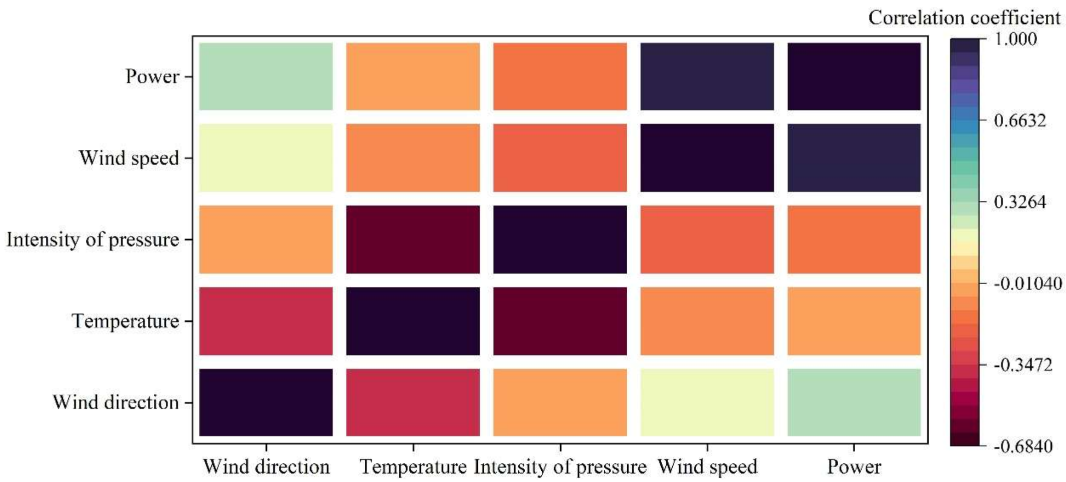

Fig. 3. The correlation between NWP and power

Because the superposition of the four numerical weather forecasts covers the spatial physical properties of the whole wind farm, the four-dimensional matrix obtained in this paper by weighting them by their correlation with the power generation is the spatio-temporal characteristic matrix. The four dimensions of the four-dimensional matrix are: the characteristic time series, the spatial distribution of the field stations, the NWP meteorological elements and the wind power clusters. Since the data set used in this paper is only one field cluster of a wind farm in Province J, and the fourth dimension is 1, the three-dimensional input has the same feature map as the four-dimensional input, and this paper only discusses the case of the four-dimensional input.

In this paper, the processed data are normalized according to Eq. (14) before the prediction, and the predicted values obtained at the end of the prediction are then inversely normalized, so that the prediction results are guaranteed to be the same magnitude and range as the original data. Namely:

$$\begin{cases} \dot{Z} = \dfrac{Z_i}{Z_{Max}} \\ \hat{Z}_i = Z_{pre} \times Z_{Max} \end{cases} \tag{14}$$

where: Z_i is the actual value. $\hat{Z}$ is the normalized value. Z_{Max} is the maximum value in the wind power sequence, Z_{pre} is the predicted value, and $\hat{Z}_i$ is the inverse normalized value of the predicted value.

3.1.1. Data preparation and assessment indicators. In this paper, the coefficient of determination $\left(R^2\right)$, the root-mean-square error $\left(RMSE\right)$ and the average absolute error $\left(MAE\right)$ are used as the evaluation indexes to evaluate the results of the inverse normalized wind power prediction, and the specific expressions of the above evaluation indexes are as follows:

$$E_{RMSE} = \sqrt{\frac{1}{n}\sum_{i=1}^{n}\left(\frac{P_{Pi}-P_{Mi}}{C}\right)^2} \tag{15}$$

$$E_{MAE} = \frac{1}{n}\sum_{i=1}^{n}\left|\frac{P_{Pi}-P_{Mi}}{C}\right| \tag{16}$$

$$R^2 = 1-\frac{\sum_{i=1}^{n}\left(P_{Mi}-P_{Pi}\right)^2}{\sum_{i=1}^{n}\left(P_{Pi}-\bar{P}_{Pi}\right)^2} \tag{17}$$

In order to test and illustrate the prediction performance of Logistic-LSTM-GCN network, the algorithms such as Extreme Gradient Boosting Decision Tree (EGBDT), Least Absolute Value Convergence and Selection Operator Algorithm (LASSO), LSTM, Gated Recurrent Unit (GRU), and TCN-LSTM are used in this paper for comparison.

3.1.2. Analysis of experimental results. According to the data prepared above are input into the Logistic-LSTM-GCN model proposed in this paper and five commonly used models, namely, LASSO, XGboost, LSTM, GRU, and TCN-LSTM, respectively, to make predictions, and a comparison of the prediction results of different models is shown in Figure 4.

Compared with other models, the predicted values of the Logistic-LSTM-GCN model proposed in this paper are the closest to the real values, and the prediction error is smaller.

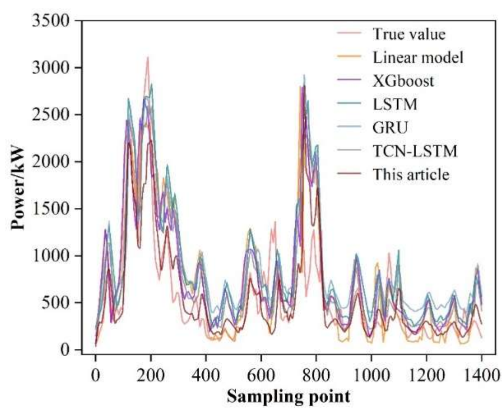

Fig. 4. Compared with other model predictions

The specific error metrics RMSE, MAE, and R^2 of the different models are compared as shown in Table 1. The proposed Logistic-LSTM-GCN prediction model in this paper has the lowest MAE and RMSE and the highest R^2 among all the models, and its MAE is reduced by an average of 2.91% and 3.40% compared to LASSO and XGboost, respectively.The RMSE is reduced by an average of 1.30% and 1.98% compared to LASSO and XGboost, respectively. R^2, on the other hand, improved by 13.61% and 16.70% on average, respectively. Comparing with LSTM, GRU and TCN-LSTM, the MAE is reduced by 5.28%, 6.03% and 3.34% on average, respectively. RMSE was reduced by an average of 3.06%, 5.63% and 3.82%, respectively. R^2 improved by 29.38%, 37.45% and 20.59% on average, respectively. This shows that the Logistic-LSTM-GCN network model used in this paper extracts the spatio-temporal information of wind farms more effectively and improves the wind cluster power prediction accuracy.

Table 1. Comparison of different model

Error index	MAE	RMSE	R^2
LASSO	0.0625	0.0719	0.6615
XGboost	0.0674	0.0787	0.6306
GRU	0.0862	0.0895	0.5038
LSTM	0.0937	0.1152	0.4231
TCN-LSTM	0.0668	0.0971	0.5917
Logistic-LSTM-GCN	0.0334	0.0589	0.7976

Meanwhile, in order to verify whether the model in this paper has effectively extracted the high-dimensional spatio-temporal information, the input features are classified into three kinds, and the one-dimensional input matrix with only wind speed as the input, the two-dimensional input matrix with the addition of station information, and the four-dimensional input matrix with the addition of spatio-temporal correlation features are modeled and predicted respectively. A comparison of the prediction results for different inputs to the model is shown in Figure 5.

The predicted values of wind power when the model inputs are 3D/4D spatio-temporal features are the closest to the real values, i.e., the best prediction of wind power.

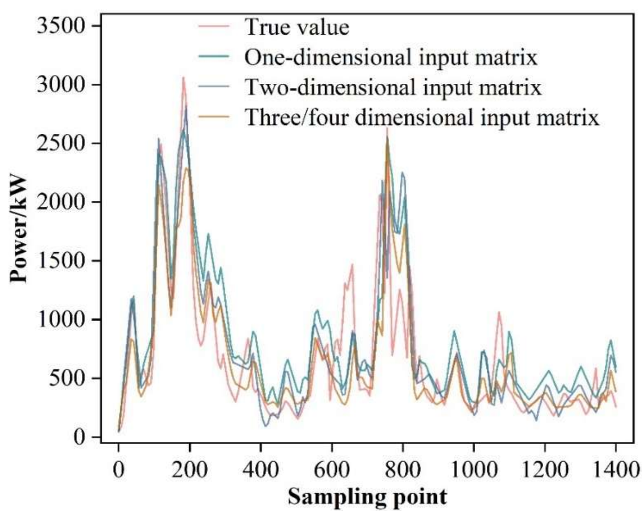

Fig. 5. Comparison of prediction results of different input models

The various prediction error metrics under different inputs of the model are shown in Table 2. The results show that the model prediction with four-dimensional spatio-temporal feature matrix inputs reduces the RMSE by 1.93% and 0.89% on average compared with the models with one-dimensional and two-dimensional inputs, and the MAE reduces by 2.38% and 0.93% on average, and the R^2 improves by 17.70% and 14.59% on average, respectively. Therefore, it can be concluded that the Logistic-LSTM-GCN model based on spatio-temporal information can effectively extract the spatio-temporal features of wind power clusters and improve the model accuracy.

Table 2. Comparison of different input model

Error index	MAE	RMSE	R^2
One-dimensional input	0.0605	0.0852	0.6356
Two-dimensional input	0.0501	0.0707	0.6667
Three/four dimensional input	0.0412	0.0614	0.8126

3.2. Model Testing and Analysis

In order to further validate the prediction performance of the Logistic-LSTM-GCN model, the prediction error test is conducted in this paper in terms of both time step and unit characteristics, respectively.

3.2.1. Evaluation indicators. The size of the error represents the closeness of the predicted value to the actual value, and the indicators involved in the analysis in this section include the average absolute error (MAE), the average absolute percentage error $(MAPE)$, and the root-mean-square error $(RMSE)$.

The value of $RMSE$ is the open root of the mean square error, which makes the value of the error after the open root smaller, and is mainly used to reflect the prediction, the actual value of the deviation. $RMSE$ expression is shown in equation (18):

$$RMSE = \sqrt{\frac{1}{N}\sum_{i=1}^{N}\left(\hat{y}_i - y_i\right)^2} \tag{18}$$

3.2.2. Prediction Error Testing and Analysis for Different Time Steps. Since the ultra-short-term prediction of wind power at different time steps has different significance for WTGs as well as for wind power grid integration, in this section, the prediction of wind power at steps of 1~9s is performed respectively. The training data used comes from the wind turbine operation data of a certain model from a wind farm in a certain place, and the data is cleaned and interpolated, and the input data is adjusted to the input vector format according to the data structure, and inputted into the prediction model for prediction. The data used to train the model has a sample size of 2.5 million and the data used to test the model has a sample size of 500.

The prediction error statistics for input vectors with different time steps are shown in Table 3. Since wind speed is a strongly correlated feature of wind power, in order to further explore the effect of wind speed on wind power prediction, the wind speed is decomposed in this paper, so the types of input data for the model in this section include wind speed, wind speed decomposition component, rotor speed, yaw error, and wind direction.

Comparing the error metrics in Table 3, longitudinally, all error metrics are gradually increasing as the time step continues to increase. Comparing the MAE metrics, from 1s to 9s, the MAE error per time step increases by 2.11KW, 3.35KW, 2.42KW, 0.76KW, 0.65KW, 1.02KW, 1.43KW, and 2.36KW, respectively, the RMSE error increases by 2.86KW, 5.10KW, 1.96KW, 2.41KW, 0.75KW, 1.65KW, 2.44KW, and 3.22KW, and the MAPE error increases by 0.26%, 0.42%, 0.18%, 0.45%, 0.11%, 0.18%, 0.09%, and 0.25%, respectively.

Table 3. Prediction error of different time steps

Time step	Error index		
	MAE/kW	RMSE/kW	MAPE/%
1s	12.13	15.79	1.56
2s	14.24	18.65	1.82
3s	17.59	23.75	2.24
4s	20.01	25.71	2.42
5s	20.77	28.12	2.87
6s	21.42	28.87	2.98
7s	22.44	30.52	3.16
8s	23.87	32.96	3.25
9s	26.23	36.18	3.50

The comparison of the wind power prediction results for 1~3s, 4-6s, and 7-9s are shown in Fig. 6 (a)~(c), respectively. As can be seen from Fig. 6, the gradual increase of the error index is presented in the curve graph, i.e., the fitting degree for the actual power curve graph becomes worse. The reason for analyzing the gradual increase of the error is that the training prediction with known data, for the current moment, the closer the moment the more accurate the prediction accuracy, the further the moment because of a variety of operational status and environmental changes, the existing data can not learn the characteristics of the information at that time, it will cause inaccuracy of prediction, prediction error becomes larger. Therefore, as the time step increases, the further away the moment to be predicted, the higher the prediction error obtained. Meanwhile, for the same prediction model, the prediction accuracies of different time steps are relatively high although they change, which indicates that the established prediction model has some applicability at different time steps.

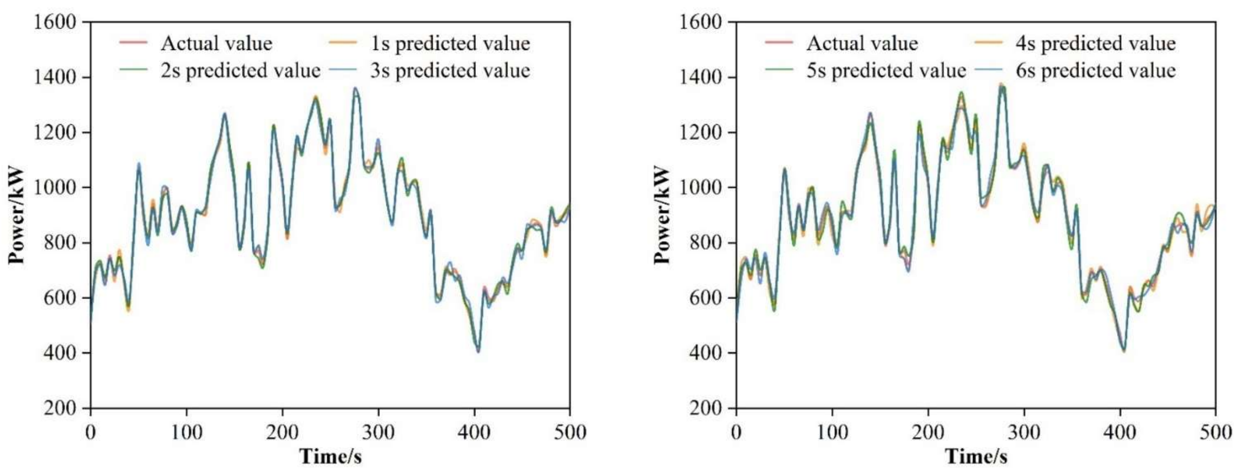

(a)1~3s (b)4~6s

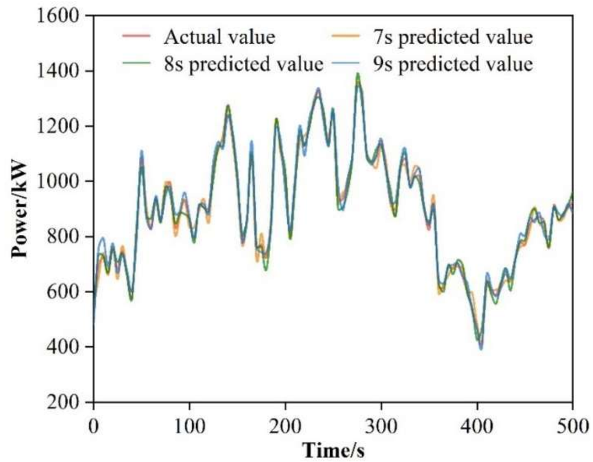

(c)7~9s

Fig. 6. Comparison of wind power prediction results

3.2.3. Prediction Error Testing and Analysis for Different Unit Characteristics. In order to verify the effect of the input of different unit state quantities on the prediction accuracy, the prediction accuracies in the case of adding different unit state quantities are tested and compared. In order to verify the effect of the frequency component of the wind speed decomposition on the prediction accuracy, the accuracy of the prediction using the wind speed directly and the prediction using the decomposed wind speed are compared.

The prediction errors of the model input data with different unit characteristics are shown in Table 4, where the error data are trained based on the Logistic-LSTM-GCN model, 2.5 million data samples are used for the training of the model, 500 data samples are used for the testing of the model, and the prediction results are taken as 4s as the time step. In the table, DWS stands for decomposed wind speed component, YE stands for yaw error, WD stands for wind direction, RS stands for rotor speed, and WS stands for undecomposed wind speed. DWS+YE means that the input vector includes decomposed wind speed and yaw error. DWS+YE+WD means that the input vector is added with the wind direction on top of DWS+YE, and the input vector includes decomposed wind speed, yaw error and wind direction. Similarly, DWS+YE+WD+RS means that the input vector includes the decomposed wind speed, yaw error, wind direction, and rotor speed, and WS+YE+WD+RS means that the input vector includes the undecomposed wind speed, yaw error, wind direction, and rotor speed.

First, the impact of model inputs of different unit state quantities on the prediction accuracy is analyzed, and the input vectors are DWS, DWS+YE, DWS+YE+WD, and DWS+YE+WD+RS, respectively, and test comparisons are performed, and the graphs of the power prediction results for the inputs of different unit state quantities are shown in Fig. 7. Legends D, DY, DYW, and DYWR in the figure are abbreviations for DWS, DWS+YE, DWS+YE+WD, and DWS+YE+WD+RS, respectively.

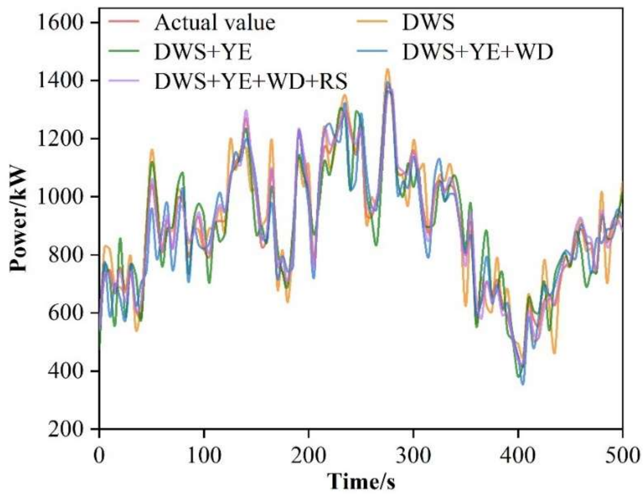

Fig. 7. Input power prediction results of different unit state quantities

Comparing the three prediction error metrics of MAE, RMSE, and MAPE for different unit state volume inputs, the DWS+YE with yaw error added to the input data is reduced by 2.17 KW, 1.27 KW, and 0.19%, respectively, compared to the DWS with only the decomposed wind speed component. DWS+YE+WD is 0.91KW, 0.21KW and 0.23% less than DWS+YE and 3.08KW, 1.48KW and 0.42% less than DWS. DWS+YE+WD+RS is 42.90KW, 57.59KW and 5.66% less than DWS+YE+WD and 45.98KW, 59.07KW and 6.08% less than DWS. As more state quantities related to unit operation are input to the model, the error gradually decreases and the prediction becomes more and more effective. And the prediction accuracy is significantly improved after the rotor speed is added to the input data. The reason is that, in addition to the main relationship between the generating power of the unit and the wind speed, there are also some state quantities affecting the operation, such as the wind direction, yaw error, etc. These state quantities affect the process of converting the wind speed into power, and taking them into account in the model can make the prediction model fit the actual situation better. At the same time, the current rotational speed of the unit reflects the current moment of inertia and the operating state at this time, and the current yaw error and the current wind direction of the unit also have a strong correlation with the unit's power generation efficiency. The rotor speed is directly related to the operation state, which more directly reflects the actual situation, making the addition of rotor speed more obvious to improve the prediction accuracy.

Table 4. Prediction error of different time steps

Input volume	Error index		
	MAE/kW	RMSE/kW	MAPE/%
DWS	68.35	87.42	8.91
DWS+YE	66.18	86.15	8.72
DWS+YE+WD	65.27	85.94	8.49
DWS+YE+WD+RS	22.37	28.35	2.83
WS+YE+WD+RS	41.65	52.13	5.36

To analyze the effect of decomposition of wind speed on wind power prediction, DWS+YE+WD+RS is tested and compared with WS+YE+WD+RS. The results of wind speed decomposition and undecomposed power prediction are shown in Fig. 8.

From Table 4, it can be seen that the MAE, RMSE, and MAPE indexes of DWS+YE+WD+RS are reduced by 19.28 KW, 23.78 KW, and 2.53%, respectively, compared to WS+YE+WD+RS. Meanwhile, observation of Fig. 8 shows that the fitting of WS+YE+WD+RS is not as effective as DWS+YE+WD+RS in some local extreme parts. The reason for this is that the input of DWS contains wind speed decomposition components, which contain high-frequency information of wind speed, and the learnable information in the local extreme value part is significant, which makes the model can learn directly, and the obtained prediction accuracy is higher and the fitting effect is better.

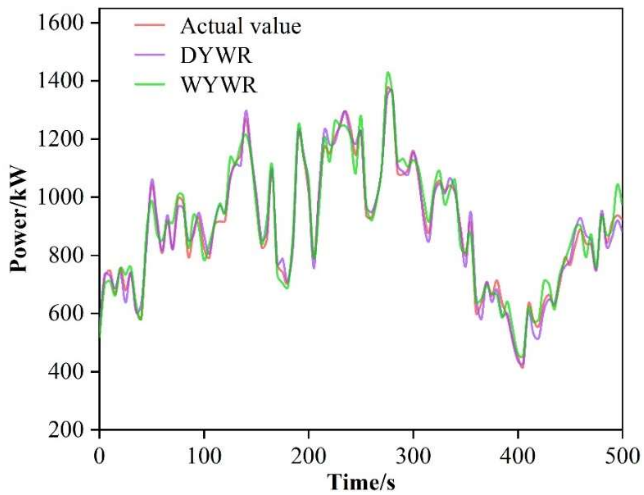

Fig. 8. Wind velocity decomposition and undecomposed power prediction results

4. Conclusion

In this paper, a multivariate wind power ultra-short-term power prediction model coupled with LSTM, Logistic, and GCN is constructed, and the performance of the model is tested.

1) The correlation between four weather features, namely wind speed, wind direction, pressure, and temperature, and the predicted wind power is analyzed. The strong correlation feature screened is wind speed, while wind direction, pressure and temperature are all weakly correlated features. Thus, wind speed is used as the third dimension of the input data, and wind direction, pressure and temperature are normalized and weighted according to the magnitude of correlation as the third dimension of the input data.

2) Compare the performance of the proposed Logistic-LSTM-GCN prediction model with LASSO, XGboost, LSTM, GRU, and TCN-LSTM, and the MAE, RMSE, and R^2 of the Logistic-LSTM-GCN model are 3.34%, 5.89%, and 79.76% respectively, which are smaller than those of the other models, while the R^2 values are all larger than other models, indicating that the model in this paper can effectively extract the spatio-temporal information of wind farms and improve the power prediction accuracy of wind power clusters. Meanwhile, under different input cases, the prediction error of this paper's model with four-dimensional spatio-temporal feature matrix is the smallest and the prediction accuracy is the highest, which in turn verifies the effectiveness of the model.

3) Analyze the effects of time step and unit characteristics on model prediction performance. With the increasing time step, all the error indicators are gradually increasing. Comparing the MAE indicators, from 1s to 9s, the values of the error indicators MAE, RMSE, and MAPE gradually increase. It indicates that as the time step increases, the moment to be predicted is farther away, and the prediction error obtained is higher. Meanwhile, the prediction accuracy of the model in this paper still maintains a high level in general, indicating that the established prediction model has some applicability at different time steps. In addition, the values of MAE, RMSE, and MAPE decrease gradually with the increase of the input types of unit state quantities, such as wind speed, yaw error, wind direction, and rotor speed, indicating that these state quantities affect the process of converting the wind speed into power, and they should be taken into account in the model so that the prediction model can better fit the actual situation, and accurate ultra-short-term prediction of wind power can

be carried out.

References

[1] Barra, P. H., de Carvalho, W. C., Menezes, T. S., Fernandes, R. A. S., & Coury, D. V. (2021). A review on wind power smoothing using high-power energy storage systems. Renewable and Sustainable Energy Reviews, 137, 110455.

[2] Ma, J., Yang, M., & Lin, Y. (2019). Ultra-short-term probabilistic wind turbine power forecast based on empirical dynamic modeling. IEEE Transactions on Sustainable Energy, 11(2), 906-915.

[3] Wu, Q., Guan, F., Lv, C., & Huang, Y. (2021). Ultra-short-term multi-step wind power forecasting based on CNN-LSTM. IET Renewable Power Generation, 15(5), 1019-1029.

[4] Wei, J., Wu, X., Yang, T., & Jiao, R. (2023). Ultra-short-term forecasting of wind power based on multi-task learning and LSTM. International Journal of Electrical Power & Energy Systems, 149, 109073.

[5] Ju, Y., Sun, G., Chen, Q., Zhang, M., Zhu, H., & Rehman, M. U. (2019). A model combining convolutional neural network and LightGBM algorithm for ultra-short-term wind power forecasting. Ieee Access, 7, 28309-28318.

[6] Che, J., Yuan, F., Deng, D., & Jiang, Z. (2023). Ultra-short-term probabilistic wind power forecasting with spatial-temporal multi-scale features and K-FSDW based weight. Applied Energy, 331, 120479.

[7] Xiang, L., Liu, J., Yang, X., Hu, A., & Su, H. (2022). Ultra-short term wind power prediction applying a novel model named SATCN-LSTM. Energy Conversion and Management, 252, 115036.

[8] Li, Y., Wang, H., Yan, J., Ge, C., Han, S., & Liu, Y. (2024). Ultra-short-term wind power forecasting based on the strategy of "dynamic matching and online modeling". IEEE Transactions on Sustainable Energy.

[9] Hu, C., Zhao, Y., Jiang, H., Jiang, M., You, F., & Liu, Q. (2022). Prediction of ultra-short-term wind power based on CEEMDAN-LSTM-TCN. Energy Reports, 8, 483-492.

[10] Zha, W., Liu, J., Li, Y., & Liang, Y. (2022). Ultra-short-term power forecast method for the wind farm based on feature selection and temporal convolution network. ISA transactions, 129, 405-414.

[11] Fan, H., Zhen, Z., Liu, N., Sun, Y., Chang, X., Li, Y., ... & Mi, Z. (2023). Fluctuation pattern recognition based ultra-short-term wind power probabilistic forecasting method. Energy, 266, 126420.

[12] Wang, F., Tong, S., Sun, Y., Xie, Y., Zhen, Z., Li, G., ... & Liu, D. (2022). Wind process pattern forecasting based ultra-short-term wind speed hybrid prediction. Energy, 255, 124509.

[13] Wei, W., Zhang, Y., Wu, G., & Tong, M. (2012, May). Ultra-short-term/short-term wind power continuous prediction based on fuzzy clustering analysis. In IEEE PES Innovative Smart Grid Technologies (pp. 1-6). IEEE.

[14] Yang, M., Guo, Y., & Huang, Y. (2023). Wind power ultra-short-term prediction method based on NWP wind speed correction and double clustering division of transitional weather process. Energy, 282, 128947.

[15] Fang, R., Wang, Y., Shang, R., Liang, Y., Wang, L., & Peng, C. (2016). The ultra-short term power prediction of wind farm considering operational condition of wind turbines. International Journal of Hydrogen Energy, 41(35), 15733-15739.

[16] Hong, D. Y., Ji, T. Y., Li, M. S., & Wu, Q. H. (2019). Ultra-short-term forecast of wind speed and wind power based on morphological high frequency filter and double similarity search algorithm. International Journal of Electrical Power & Energy Systems, 104, 868-879.

[17] Ji, T., Jiang, Y., Li, M., & Wu, Q. (2022). Ultra-short-term wind speed and wind power forecast via selective Hankelization and low-rank tensor learning-based predictor. International Journal of Electrical Power &

Energy Systems, 140, 107994.

[18] Tan, B., Ma, X., Shi, Q., Guo, M., Zhao, H., & Shen, X. (2021, September). Ultra-short-term wind power forecasting based on improved LSTM. In 2021 6th International Conference on Power and Renewable Energy (ICPRE) (pp. 1029-1033). IEEE.

[19] Liu, L., Liu, J., Ye, Y., Liu, H., Chen, K., Li, D., ... & Sun, M. (2023). Ultra-short-term wind power forecasting based on deep Bayesian model with uncertainty. Renewable Energy, 205, 598-607.

[20] Yu, G. Z., Lu, L., Tang, B., Wang, S. Y., & Chung, C. Y. (2022). Ultra-short-term wind power subsection forecasting method based on extreme weather. IEEE Transactions on Power Systems, 38(6), 5045-5056.

[21] Ma, J., Yang, M., Han, X., & Li, Z. (2017). Ultra-short-term wind generation forecast based on multivariate empirical dynamic modeling. IEEE Transactions on Industry Applications, 54(2), 1029-1038.

[22] Yang, S., Yuan, A., & Yu, Z. (2023). A novel model based on CEEMDAN, IWOA, and LSTM for ultra-short-term wind power forecasting. Environmental Science and Pollution Research, 30(5), 11689-11705.

[23] Li, C., Cao, D. S., Zhao, Z. T., Wang, X., & Xie, X. Y. (2024). Forecast for wind power at ultra-short-term based on a composite model. Energy Reports, 12, 4076-4082.

[24] Sawant, M., Patil, R., Shikhare, T., Nagle, S., Chavan, S., Negi, S., & Bokde, N. D. (2022). A selective review on recent advancements in long, short and ultra-short-term wind power prediction. Energies, 15(21), 8107.

[25] Yu, G., Shen, L., Dong, Q., Cui, G., Wang, S., Xin, D., ... & Lu, W. (2024). Ultra-short-term wind power forecasting techniques: comparative analysis and future trends. Frontiers in Energy Research, 11, 1345004.

[26] Sun, Y., Li, Z., Yu, X., Li, B., & Yang, M. (2020). Research on ultra-short-term wind power prediction considering source relevance. Ieee Access, 8, 147703-147710.

[27] Li, J., Geng, D., Zhang, P., Meng, X., Liang, Z., & Fan, G. (2019, September). Ultra-short term wind power forecasting based on LSTM neural network. In 2019 IEEE 3rd International Electrical and Energy Conference (CIEEC) (pp. 1815-1818). IEEE.

[28] Kai Chen, Roberto Cudmani& Andres Alfonso Pena Olarte. (2024). Validation of a damage constitutive model based on logistic model dedicated to the mechanical behavior of the rock. Geomechanics and Geophysics for Geo-Energy and Geo-Resources(1),15-15.

[29] Ali Rizwan, Xu Jin, Baig Mushahid Hussain, Rehman Hafiz Saif Ur, Waqas Aslam Muhammad & Qasim Kaleem Ullah. (2024). From data to decisions: enhancing financial forecasts with LSTM for AI token prices. Journal of Economic Studies(8),1677-1693.

[30] Veeramani Mangala Gowri, Ajay Ajith, P. Senthil Kumar, Tanawat Imboon, S. Abraham John, Sirikanjana Thongmee & Gayathri Rangasamy. (2024). Anisotropic gold nanostructure-mediated electrocatalysis on exfoliated GCN: A shape-dependent study. Surfaces and Interfaces105453-105453.